Variational calculation of neoclassical ion heat flux and poloidal flow in the banana regime for axisymmetric magnetic geometry

2012 Plasma Phys. Control. Fusion 54 085011

(http://iopscience.iop.org/0741-3335/54/8/085011)

IOP Publishing Plasma Physics and Controlled Fusion
Plasma Phys. Control. Fusion **54** (2012) 085011 (8pp) doi:10.1088/0741-3335/54/8/085011

Variational calculation of neoclassical ion heat flux and poloidal flow in the banana regime for axisymmetric magnetic geometry

Jeffrey B Parker[1] **and Peter J Catto**[2]

[1] Princeton University, Princeton, NJ 08544, USA
[2] Plasma Science and Fusion Center, Massachusetts Institute of Technology, Cambridge, MA 02139, USA

Received 29 December 2011, in final form 3 April 2012
Published 3 July 2012
Online at stacks.iop.org/PPCF/54/085011

Abstract
We present a numerical solution of the drift-kinetic equation retaining the linearized Fokker–Planck collision operator which is valid for general axisymmetric magnetic geometry in the low collisionality limit. We use the well-known variational principle based on entropy production and expand in basis functions. Uniquely, we expand in pitch-angle basis functions which are eigenfunctions of the transit-averaged test particle collision operator. These eigenfunctions, which depend on the geometry, are extremely well suited to this problem, with only one or two basis functions required to obtain an accurate solution. As a simple example of the technique, the neoclassical ion heat flux and poloidal flow are calculated for circular flux surfaces and compared with analytic approximations for arbitrary aspect ratio.

(Some figures may appear in colour only in the online journal)

1. Introduction

Neoclassical transport is concerned with the transport of particles, heat, momentum and current due to collisional relaxation in an inhomogeneous magnetic geometry [1, 2]. Usually, neoclassical cross-field transport is overwhelmed by turbulent transport. However, under enhanced confinement conditions such as within an internal transport barrier, turbulence can be suppressed and ion thermal transport can be reduced to neoclassical levels [3]. As a result, there has been a revival of interest in accurate calculations of neoclassical transport.

Numerical solutions of the drift-kinetic equation (DKE) have been carried out previously. The NEO code by Belli and Candy calculates neoclassical transport for arbitrary collisionality including multiple species [4]. The NEO code has recently been upgraded to incorporate the full linearized Fokker–Planck collision operator [5]. The NCLASS code [6] is similar, though in that work collisions are incorporated through the Hirshman–Sigmar approximation [7] to the linearized Fokker–Planck collision operator. Recently, Wong and Chan have also solved the first order DKE for a single ion species and arbitrary collisionality using the full linearized Fokker–Planck collision operator [8]. However, their technique converges too slowly in the limit of low collisionality and large aspect ratio to compare with the available exact results.

In this work we solve the first order ion DKE for a single ion species in the low collisionality limit using the full linearized Fokker–Planck operator. Our solution method uses a variational principle [9] for the first order DKE and is valid in arbitrary axisymmetric magnetic geometry. Uniquely, we use an expansion in pitch-angle basis functions which are eigenfunctions of the transit-averaged test particle collision operator [10–12]. These eigenfunctions, which depend on the geometry, turn out to be extremely well suited to this problem. Because we are considering weak collisionality, and not considering finite orbit width effects or coupling with electrons or impurities, our work should be viewed as a study of the importance of keeping the linearized Fokker–Planck collision operator without approximation. We emphasize that our method is not intended to compete with the general codes

such as NEO. Instead our aims are to provide a simple method of calculation in the collisionless limit and also to demonstrate the utility of the pitch-angle eigenfunctions.

Our solution easily converges to the known results in the limit of large aspect ratio and unit aspect ratio. For concentric circular flux surfaces, we find that at intermediate aspect ratios, the well-known approximate analytic expressions accurately calculate the ion heat flux, but there are small corrections required for plasma flow.

2. Variational principle

To examine the consequences of retaining the full linearized Fokker–Planck collision operator we work in the limit of small gyroradius and small normalized collisionality and retain a single ion species. The starting point for the theory is the DKE for the gyroaveraged ion distribution function f [1]. The primary ordering parameter is $\delta \equiv \rho/L$, where $\rho = v_\mathrm{T}/\Omega$ is the gyroradius, L is the macroscopic scale length, $v_\mathrm{T} = (2T/m)^{1/2}$ is the thermal speed, $\Omega = ZeB/mc$ is the gyrofrequency, T is the ion temperature, Z and m are the ion charge number and mass, respectively, B is the magnetic field, and c is the speed of light. The equilibrium magnetic field is $\boldsymbol{B} = \nabla\zeta \times \nabla\psi + I(\psi)\nabla\zeta$ where ζ is the toroidal angle, ψ is the poloidal flux divided by 2π, $I = RB_\zeta$, and R is the major radius.

After expanding in small δ, H-theorem arguments show that the lowest order distribution is Maxwellian on each flux surface, $f_m = n/(\pi^{3/2}v_\mathrm{T}^3)\exp(-v^2/v_\mathrm{T}^2)$, where n is the ion density [1]. The small δ ordering implies behavior is local in ψ. The steady-state DKE written for the perturbed ion distribution function f_1 can be written

$$v_\parallel \nabla_\parallel f_1 + \boldsymbol{v}_\mathrm{d}\cdot\nabla f_m = C(f_1), \tag{1}$$

or equivalently,

$$v_\parallel \nabla_\parallel \left(f_1 + \frac{I v_\parallel}{\Omega}\left.\frac{\partial f_m}{\partial \psi}\right|_E \right) = C(f_1), \tag{2}$$

where $f = f_m + f_1$, $\boldsymbol{v}_\mathrm{d}$ is the guiding center drift, C is the linearized like-species Fokker–Planck collision operator, and the gradients and ψ derivative are performed at constant energy (see, e.g., [1, p 260]). We neglect ion–electron collisions. Subsidiary expansion is performed in the limit of small normalized collisionality ν_*, where $\nu_* = \nu_\mathrm{eff}/\omega_\mathrm{b}$, ν_eff is the effective scattering frequency of trapped particles, and ω_b is the bounce frequency of trapped particles. One obtains the 'collisional constraint equation' for the perturbed distribution function [1, 9, 13]

$$\left\langle \frac{B}{v_\parallel} C(f_1) \right\rangle = 0. \tag{3}$$

The angle brackets denote a poloidal transit average, given by $\langle y\rangle = \left(\oint \mathrm{d}\theta\, y/\boldsymbol{B}\cdot\nabla\theta\right) / \int_0^{2\pi} \mathrm{d}\theta/\boldsymbol{B}\cdot\nabla\theta$, where θ is the poloidal angle. The integral in the numerator goes from 0 to 2π for untrapped particles and is a closed orbit between the turning points for trapped particles. We decompose f_1 as

$$f_1 \equiv F + g, \tag{4}$$

where F is a known function and acts as a source term, and is given by

$$F = -\frac{I v_\parallel}{\Omega}\left.\frac{\partial f_m}{\partial \psi}\right|_E = -\frac{I v_\parallel}{\Omega}\left[\frac{p'}{p} + \frac{q\Phi'}{T} + \left(\frac{v^2}{v_\mathrm{T}^2} - \frac{5}{2}\right)\frac{T'}{T}\right] f_m. \tag{5}$$

Here the ψ derivative is taken at constant total energy $E = mv^2/2 + Ze\Phi$, Φ is the electric potential, p is the ion pressure and a prime denotes $\mathrm{d}/\mathrm{d}\psi$. The unknown function to be solved for is g, which depends only on constants of the motion and not on θ [9]. The homogeneous solutions of equation (3) which may be added to g amount to a shift in the density or temperature of the full distribution function, so such homogeneous solutions are ignored. The integral in equation (3) annihilates the drive term F in the trapped region of phase space, and so g is zero in the trapped region. A consequence of the above is that g has a discontinuous derivative at the trapped-passing boundary. It has been shown that if one goes to next order in collisionality ν_*, in actuality a boundary layer exists, and the discontinuity can be resolved [14].

A variational principle for the collisional constraint equation is given by the minimization of the entropy production integral [1, 9, 13]

$$S = -\left\langle \int \mathrm{d}^3 v \frac{f_1}{f_m} C(f_1) \right\rangle. \tag{6}$$

To solve the collisional constraint equation, we can in principle evaluate equation (6) for many different trial functions f_1. If the trial functions are chosen well, the f_1 which gives the lowest value for S is closest to the true solution and presumably a good approximation. The trial functions are constrained by equation (4) and the vanishing of g in the trapped region. Because the drive term is odd in $v_\parallel$, it is also clear that g will be odd in $v_\parallel$.

One way to parametrize the search space of all allowable functions g is to write g as an expansion in basis functions. For this purpose we use the velocity coordinates (x, λ, σ), where $x \equiv v/v_\mathrm{T}$, $\lambda \equiv v_\perp^2 B_\mathrm{max}/v^2 B$, $\sigma \equiv \mathrm{sign}(v_\parallel)$ and B_max is the maximum magnetic field on a flux surface. We write g and f_1 in the following normalized form:

$$g = A f_m \sum_i a_i B_i(x, \lambda, \sigma), \tag{7}$$

$$f_1 = A\left(\sum_i a_i B_i(x,\lambda,\sigma) - h x^3 \xi\right) f_m - \frac{I v_\parallel}{\Omega}\left[\frac{p'}{p} + \frac{q\Phi'}{T} - \frac{5}{2}\frac{T'}{T}\right] f_m, \tag{8}$$

where $\xi = v_\parallel/v$, $A \equiv I v_\mathrm{T} T'/\Omega_\mathrm{max} T$, $\Omega_\mathrm{max} \equiv ZeB_\mathrm{max}/mc$, $\kappa \equiv n/(\pi^{3/2}v_\mathrm{T}^3)$ is defined through $f_m = \kappa \mathrm{e}^{-x^2}$ and $h(\theta) \equiv B_\mathrm{max}/B(\theta)$. The basis functions B_i satisfy the same constraints as g, namely they vanish in the trapped region and are odd in σ. The a_i are the unknown coefficients. Equation (6) becomes

$$\eta^{-1} S = -\left\langle \int \mathrm{d}^3 x \frac{f_1}{f_m}\frac{C(f_1)}{A^2 \kappa \nu_\mathrm{B}} \right\rangle, \tag{9}$$

where $\eta \equiv A^2\pi^{-3/2}n\nu_B$ and $\nu_B = 4\sqrt{\pi}Z^4e^4n\ln\Lambda_c/3\sqrt{m}T^{3/2}$ is the Braginskii collision frequency. We substitute equation (8) into equation (9) and recognize that due to the conservation properties of the collision operator, the terms in square brackets in equation (8) are annihilated by the integral. We obtain

$$\eta^{-1}S = -\sum_{i,j} a_i a_j M_{ij} + 2\sum_i a_i b_i - \left\langle h^2 \int d^3x\, x^3\xi \widehat{C}_n\left(x^3\xi\right)\right\rangle, \tag{10}$$

where $\widehat{C}_n \equiv \widehat{C}/(\kappa\nu_B)$ is the normalized collision operator, $\widehat{C}(\chi) \equiv C(\chi f_m)$, and self-adjointness has been used. The matrix elements are given by

$$M_{ij} \equiv \left\langle \int d^3x\, B_i \widehat{C}_n(B_j)\right\rangle, \tag{11}$$

$$b_i \equiv \left\langle h\int d^3x\, B_i\widehat{C}_n\left(x^3\xi\right)\right\rangle = h\int d^3x\, B_i\widehat{C}_n\left(x^3\xi\right), \tag{12}$$

where M is a symmetric matrix as a result of self-adjointness. The second form of b_i without an explicit flux surface average holds because there is no θ dependence left over when the velocity integral is done first. In matrix notation,

$$\eta^{-1}S = -a^T M a + 2a^T b + \eta^{-1}S_3, \tag{13}$$

where

$$\eta^{-1}S_3 \equiv -\left\langle h^2\int d^3x\, x^3\xi\widehat{C}_n\left(x^3\xi\right)\right\rangle = \pi^{3/2}\left\langle h^2\right\rangle. \tag{14}$$

In evaluating equation (14) we used

$$d^3x = dx\, d\lambda\, d\varphi \sum_\sigma x^2/2h|\xi| \tag{15}$$

and

$$\frac{\widehat{C}_n(x^3\xi)}{\xi} = -\frac{30xe^{-2x^2} + 3e^{-x^2}\sqrt{\pi}(-5+2x^2)\mathrm{erf}(x)}{\sqrt{2}x^2}, \tag{16}$$

the latter of which is independent of ξ due to the rotational symmetry of C.

We can minimize S in equation (10) with respect to each of the a_i by taking the partial derivative $\partial/\partial a_i$ and setting it equal to 0, which yields a matrix equation for the coefficients a_j,

$$Ma = b. \tag{17}$$

While we have derived this matrix equation from the variational principle, it can also be derived directly from the collisional constraint equation. The same matrix equation is obtained from equation (3) by substituting in equation (8) and applying $\sum_\sigma \sigma \int dv\, d\lambda\, v^2 B_j$.

3. Basis functions

We now turn to the question of exactly what basis function $B_i(v,\lambda,\sigma)$ to use for our expansion. Any complete set of basis functions suffices in principle, but the expansion's rate of convergence depends on the basis set. Here we describe our choice of basis set which will be seen to produce rapid convergence. We let $i \to \{l, n\}$ and use the separable form

$$B_{ln} = \sigma V_l(x) g_n(\lambda) \tag{18}$$

where $l = 0, \ldots, L$ and $n = 1, \ldots, N$.

In the Spitzer problem, a Laguerre polynomial expansion is used and only the first two source terms in this basis are nonzero; all the others vanish by orthogonality. This procedure leads to a rapid convergence of the coefficients as one increases the number of polynomials retained [13]. In the Spitzer problem, however, the source term is a polynomial in speed. In contrast, for our neoclassical problem the source term is $\widehat{C}_n(x^3\xi)/\xi$ which is a complicated function of x involving error functions and exponentials in the definition. It is too much to hope that all but a few of the source terms are zero. However, if the source terms $b_{l,n}$ decayed quickly as l or n increased, the coefficients should converge rapidly. Using equations (18) and (16) in equation (12) gives

$$b_{ln} = 2\pi\int_0^\infty dx\, x^2 V_l(x)\frac{\widehat{C}_n(x^3\xi)}{\xi}\int_0^{h_{\min}} d\lambda\, g_n(\lambda). \tag{19}$$

The x and λ integrals of b_{ln} are independent. Ideally, the λ integral tends to zero for large n, while the speed integral tends to zero for large l. This behavior will be used as a criterion for determining appropriate basis functions for expansion. For convenience let

$$X_l \equiv \int_0^\infty dx\, x^2 V_l(x)\frac{\widehat{C}_n\left(x^3\xi\right)}{\xi}, \tag{20}$$

$$\beta_n \equiv \int_0^{h_{\min}} d\lambda\, g_n(\lambda). \tag{21}$$

3.1. Basis function in x

For the speed basis functions a common choice is to involve the set of Laguerre polynomials $L_l^{(3/2)}(x^2)$. We use

$$V_l(x) = xL_l^{(3/2)}\left(x^2\right). \tag{22}$$

A generating function for the generalized Laguerre polynomials is [15]

$$s(x,z;\alpha) = \frac{e^{-xz(1-z)}}{(1-z)^{\alpha+1}} = \sum_{l=0}^\infty L_l^{(\alpha)}(x)z^l, \tag{23}$$

which implies

$$L_l^{(\alpha)}(x) = \frac{1}{l!}\frac{\partial^l s}{\partial z^l}\bigg|_{z=0}. \tag{24}$$

The generating function can be used to calculate the X_l. For $\alpha = 3/2$, we use equation (16) to find

$$q(z) \equiv \int_0^\infty dx\, x^3 s(x^2,z;3/2)\frac{\widehat{C}_n\left(x^3\xi\right)}{\xi} = 3\sqrt{\frac{\pi}{2}}z(2-z)^{-3/2} \tag{25}$$

and

$$X_l = \frac{1}{l!}\frac{d^l q}{dz^l}\bigg|_{z=0} = \frac{3}{2^l}\frac{\Gamma(l+1/2)}{\Gamma(l)}, \tag{26}$$

where $\Gamma(x)$ is the gamma function. Observe that X_l decays as 2^{-l}.

3.2. Basis function in λ

The primary requirement for the λ basis functions is that they are 0 in the trapped region. The passing region is given by $0 < \lambda < 1$, while the trapped region is given by $1 < \lambda < h_{\max}$. We will use eigenfunctions of the transit-averaged test particle collision operator. The eigenfunctions are defined through a Sturm–Liouville problem as the solutions of [10–12]

$$\frac{\mathrm{d}}{\mathrm{d}\lambda} p(\lambda) \frac{\mathrm{d}g_n}{\mathrm{d}\lambda} + \mu_n w(\lambda) g_n = 0, \tag{27}$$

where

$$p(\lambda) \equiv \lambda \langle |\xi| \rangle, \tag{28}$$

$$w(\lambda) \equiv \left\langle \frac{1}{h|\xi|} \right\rangle, \tag{29}$$

with boundary conditions $g(\lambda = 1) = 0$, and at the lower boundary $\lambda = 0$ we need only require that g_n and its derivative be finite. The μ_n are the eigenvalues. This differential equation is a singular Sturm–Liouville problem with a complete set of orthogonal eigenfunctions satisfying the boundary conditions. We additionally normalize the eigenfunctions such that $g_n(\lambda = 0) = 1$.

The g_n must be found numerically by solving the Sturm–Liouville problem. We obtain a set of orthogonal eigenfunctions $g_n(\lambda)$, $n = 1, 2, \ldots$ for which we define the following integrals:

$$M_n \delta_{nm} \equiv \int_0^1 \mathrm{d}\lambda \, w(\lambda) g_n(\lambda) g_m(\lambda), \tag{30}$$

$$\beta_n \equiv \int_0^1 \mathrm{d}\lambda \, g_n(\lambda). \tag{31}$$

From the properties of Sturm–Liouville equations, each g_n has n zeroes. Therefore, as n increases the g_n become more oscillatory, so β_n tends to decrease to 0 for large n, as desired. In the $\epsilon \to 0$ limit, the eigenfunctions are $g_n(\lambda) = P_{2n-1}(\sqrt{1-\lambda})$ with eigenvalues $\mu_n = 2n(2n-1)/4$, $\beta_n = 2\delta_{n1}/3$ and $M_n = 2/(4n-1)$, where the P_n are the Legendre polynomials [12].

These pitch-angle eigenfunctions have the advantage that they depend on the magnetic geometry, which removes the explicit geometric dependence from other parts of the calculation. In particular, the integrals involving the test part of the collision operator can be performed easily. In addition, in the large aspect ratio limit, the g_1 term dominates in an $\epsilon^{1/2}$ expansion, making the large aspect ratio limit easy to solve.

Figure 1 shows the first few eigenfunctions for the circular flux surface geometry described in equation (32) with $\epsilon = 0.3$. The first eigenfunction $g_1(\lambda)$ (blue solid line) can be compared with the λ dependence obtained when solving the collisional constraint equation with only the pitch-angle scattering collision operator. In that case the lambda dependence is given by the solution of the differential equation $(pg')' =$ constant, or $g_R(\lambda) = N_0 \int_\lambda^1 \mathrm{d}\lambda' / \langle \sqrt{1-\lambda'/h} \rangle$ (blue dashed line), where N_0 is a normalization constant. The two functions $g_1(\lambda)$ and $g_R(\lambda)$ are fairly close, and it can be shown they differ by $O(\epsilon^{1/2})$ in the large aspect ratio limit.

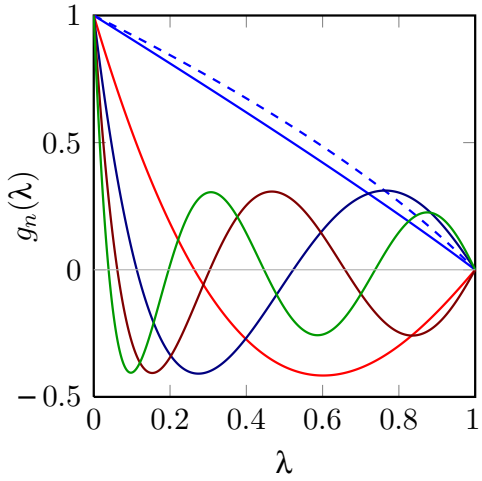

Figure 1. Pitch-angle eigenfunctions (solid lines) $g_n(\lambda)$ for $n = 1, \ldots, 5$, using the circular flux surface geometry with $\epsilon = 0.3$. The first eigenfunction $g_1(\lambda)$ is close to $g_R(\lambda)$ (dashed line), the pitch-angle dependence obtained when the collisional constraint equation is solved retaining only the pitch-angle scattering operator.

4. Solving the matrix equation

4.1. Model magnetic field

The technique as described is valid for arbitrary magnetic geometry. However, to compare with previous results, and as a particular example, we next consider a model magnetic field with concentric circular flux surfaces.

$$\boldsymbol{B} = \frac{B_{\max}(1-\epsilon)}{1+\epsilon\cos\theta} \frac{\hat{\boldsymbol{\varphi}} + k\hat{\boldsymbol{\theta}}}{\sqrt{1+k^2}}, \tag{32}$$

where k is only a function of radius. Then

$$h(\theta) = \frac{1+\epsilon\cos\theta}{1-\epsilon} \tag{33}$$

and the flux surface average of a quantity y is given by

$$\langle y \rangle = \frac{1}{2\pi} \int_0^{2\pi} \mathrm{d}\theta \, y(1+\epsilon\cos\theta). \tag{34}$$

4.2. Matrix elements

The computation of the source terms b_i has been described already in section 3. We now describe the procedure to compute the matrix elements M_{ij} in equation (11). We begin by decomposing the collision operator into the pitch-angle scattering, energy diffusion, and field terms.

$$\widehat{C}_n \equiv \widehat{C}_n^p + \widehat{C}_n^E + \widehat{C}_n^{Fa} + \widehat{C}_n^{Fb}, \tag{35}$$

where

$$\widehat{C}_n^p(\chi) = \mathrm{e}^{-x^2} |\xi| h \bar{\nu}_\perp \frac{\partial}{\partial\lambda} \lambda |\xi| \frac{\partial\chi}{\partial\lambda}, \tag{36}$$

$$\widehat{C}_n^E(\chi) = \frac{1}{2x^2} \frac{\partial}{\partial x} \mathrm{e}^{-x^2} x^4 \bar{\nu}_\parallel \frac{\partial\chi}{\partial x}, \tag{37}$$

$$\widehat{C}_n^{Fb}(\chi) = 3\sqrt{2}\mathrm{e}^{-2x^2}\chi. \tag{38}$$

The remaining part of the field operator $\widehat{C}_n^{Fa}$ is more complicated and is given shortly. Here $\bar{\nu}_\perp(x) \equiv \nu_\perp(x)/\nu_B$, $\bar{\nu}_\parallel(x) \equiv \nu_\parallel(x)/\nu_B$, $\nu_\perp(x) = \nu_B 3\sqrt{2\pi}[\mathrm{erf}(x) - \Psi(x)]/2x^3$, $\nu_\parallel(x) = \nu_B 3\sqrt{2\pi}\Psi(x)/2x^3$, $\mathrm{erf}(x)$ is the error function, and $\Psi(x) = [\mathrm{erf}(x) - x\mathrm{erf}'(x)]/2x^2$ is the Chandrasekhar function. The matrix elements involving $\widehat{C}_n^p$, $\widehat{C}_n^E$, and $\widehat{C}_n^{Fb}$ can be calculated analytically. Decomposing the M_{ij} as in equation (35) and using equations (18), (22) and (36)–(38) in (11), we obtain after some algebra

$$M_{ij}^p = \left(-\mu_n K_{ll'}^p\right) 2\pi\delta_{nn'} M_n, \tag{39}$$

$$M_{ij}^E = \left(K_{ll'}^E/2\right) 2\pi\delta_{nn'} M_n, \tag{40}$$

$$M_{ij}^{Fb} = \left(3\sqrt{2}K_{ll'}^{Fb}\right) 2\pi\delta_{nn'} M_n, \tag{41}$$

where

$$K_{ll'}^p \equiv \int_0^\infty \mathrm{d}x\, \mathrm{e}^{-x^2} x^4 \bar{\nu}_\perp L_l^{(3/2)}\left(x^2\right) L_{l'}^{(3/2)}\left(x^2\right), \tag{42}$$

$$K_{ll'}^E \equiv \int_0^\infty \mathrm{d}x\, x L_l^{(3/2)}\left(x^2\right) \times \frac{\mathrm{d}}{\mathrm{d}x}\mathrm{e}^{-x^2} x^4 \bar{\nu}_\parallel \frac{\mathrm{d}}{\mathrm{d}x}\left[x L_{l'}^{(3/2)}\left(x^2\right)\right], \tag{43}$$

$$K_{ll'}^{Fb} \equiv \int_0^\infty \mathrm{d}x\, \mathrm{e}^{-2x^2} x^4 L_l^{(3/2)}\left(x^2\right) L_{l'}^{(3/2)}\left(x^2\right). \tag{44}$$

An integration by parts could be applied to equation (43) to make the integral manifestly symmetric in l and l'. The speed integrals can be computed directly. Alternatively, the generating function technique used in section 3.1 can simplify the calculations somewhat. It is difficult to find closed-form expressions for $K_{ll'}^p$ and $K_{ll'}^E$, but it is relatively straightforward to use the generating function to find

$$K_{ll'}^{Fb} = \frac{1}{2^{7/2}} \frac{\Gamma(l + l' + 5/2)}{l!\, l'!\, 2^{l+l'}}. \tag{45}$$

The contribution to M_{ij} from the final piece of the collision operator, $\widehat{C}_n^{Fa}$, must be calculated numerically. $\widehat{C}_n^{Fa}$ is given by [16]

$$\widehat{C}_n^{Fa}(\chi) = \frac{3}{\pi\sqrt{8}}\mathrm{e}^{-x^2}\left[\frac{2v^2}{v_T^4}\frac{\partial^2 G_1}{\partial v^2} - \frac{2}{v_T^2}H_1\right], \tag{46}$$

where the Rosenbluth potentials are

$$G_1 = \int \mathrm{d}^3 v'\, f_m(v')\chi(\boldsymbol{v}')u, \tag{47}$$

$$H_1 = \int \mathrm{d}^3 v'\, f_m(v')\chi(\boldsymbol{v}')u^{-1}, \tag{48}$$

$$u = |\boldsymbol{v} - \boldsymbol{v}'|. \tag{49}$$

In normalized variables with $\boldsymbol{y} = \boldsymbol{v}'/v_T$, this becomes

$$\widehat{C}_n^{Fa}(\chi) = \frac{3}{\pi\sqrt{8}}\mathrm{e}^{-x^2}\int \mathrm{d}^3 y\, \mathrm{e}^{-y^2}\chi(\boldsymbol{y})U(u), \tag{50}$$

where now $u = |\boldsymbol{x} - \boldsymbol{y}|$ and

$$U(u) \equiv 2x^2\frac{\partial^2 u}{\partial x^2} - \frac{2}{u} = \frac{x^2 + y^2 - 2}{u} - \frac{u}{2} - \frac{\left(x^2 - y^2\right)^2}{2u^3}. \tag{51}$$

Substituting into equation (11) gives

$$M_{ij}^{Fa} = \frac{3}{\pi\sqrt{8}}\left\langle \int \mathrm{d}^3 x\, \mathrm{d}^3 y\, \sigma_x\sigma_y \mathrm{e}^{-(x^2+y^2)} g_n(\lambda_x) g_{n'}(\lambda_y) \times V_l(x) V_{l'}(y) U(u)\right\rangle. \tag{53}$$

This expression is symmetric in swapping (l, l') or (n, n') independently. That is, we not only have $M_{lnl'n'} = M_{l'n'ln}$ from self-adjointness, but we also have $M_{lnl'n'} = M_{ln'l'n}$.

In the appendix, we simplify equation (53) into a form appropriate for numerical integration.

4.3. Calculation of neoclassical quantities

Once the matrix coefficients M_{ij} have been calculated, equation (17) can be solved for the coefficients a_i. With the a_i known, the distribution function f_1 is given by equations (4) and (5) or equivalently by equation (8), and the neoclassical quantities of interest can be computed. We demonstrate the calculations of ion heat flux and plasma flow. We can relate S to the heat flux through

$$S = -\frac{1}{T^2}\frac{\mathrm{d}T}{\mathrm{d}\psi}\langle \boldsymbol{q}\cdot\nabla\psi\rangle. \tag{54}$$

After some manipulation, this yields

$$\left(\frac{nI^2}{m\Omega_{\max}^2}TT'\nu_B\right)^{-1}\langle \boldsymbol{q}\cdot\nabla\psi\rangle = -\frac{2}{\pi^{3/2}}\left(-a^T M a + 2a^T b + \pi^{3/2}\langle h^2\rangle\right) \tag{55}$$

$$= -\frac{2}{\pi^{3/2}}\left(a^T b + \pi^{3/2}\langle h^2\rangle\right). \tag{56}$$

The second line would have been obtained if we used the collisional moment expression for heat flux directly.

The poloidal flow is calculated from [13]

$$n_i v_{i\theta} = K(\psi)B_\theta, \tag{57}$$

where

$$K(\psi) \equiv \frac{1}{B}\int \mathrm{d}^3 v\, v_\parallel g. \tag{58}$$

We obtain

$$\left(\frac{nIT'}{m\Omega_{\max}B_{\max}}\right)^{-1} K = \frac{3}{2}\sum_n a_{0n}\beta_n. \tag{59}$$

The parallel flow is given by

$$n_i v_{i\parallel} = \int \mathrm{d}^3 v\, v_\parallel f_1 = -\frac{I}{m\Omega}\left(\frac{\mathrm{d}p}{\mathrm{d}\psi} + Zen\frac{\mathrm{d}\Phi}{\mathrm{d}\psi}\right) + \frac{KB}{n}. \tag{60}$$

4.4. Previous approximate analytic results

For later use in comparing with our results, we quote some previous analytic results which have been obtained approximately. The Chang–Hinton formula for ion heat flux is an interpolation between large aspect ratio and unit aspect ratio using a single approximate result at intermediate aspect ratio. Simplified to circular flux surface geometry it is [17]

$$\alpha_q^{-1}\langle \boldsymbol{q}\cdot\nabla\psi\rangle = 2\epsilon^{1/2}\left(0.66+1.88\epsilon^{1/2}-1.54\epsilon\right)\left(1+3\epsilon^2/2\right), \tag{61}$$

where $\alpha_q \equiv (nI^2TT'\nu_B/m\Omega_0^2)$, and $\Omega_0 \equiv ZeB_0/mc$ uses the magnetic field at $\theta = \pi/2$. The two field strengths B_0 and $B_{\max}$ are related by $B_{\max} = B_0 h(\pi/2)$.

Taguchi's method involves assuming a particular form for the pitch-angle dependence of g and expanding the speed dependence in Laguerre polynomials. The pitch-angle dependence is assumed to be the $g_R(\lambda)$ shown in figure 1. The Taguchi formulae for ion heat flux and poloidal flow keeping two Laguerre polynomials are [13, 18]

$$\alpha_q^{-1}\langle \boldsymbol{q}\cdot\nabla\psi\rangle = 2\left(\frac{\langle h^2\rangle}{h(\pi/2)^2}-\frac{B_0^2}{\langle B^2\rangle}\frac{f_c}{f_c+0.462f_t}\right), \tag{62}$$

$$\alpha_K^{-1}K = \frac{B_0^2}{\langle B^2\rangle}\frac{1.17f_c}{f_c+0.462f_t}, \tag{63}$$

where $\alpha_K \equiv (nIT'/m\Omega_0 B_0)$,

$$f_t \equiv 1-\frac{3}{4}\int_0^{h^h_{\min}}\frac{\lambda\,\mathrm{d}\lambda}{\langle\sqrt{1-\lambda/h^h}\rangle}, \tag{64}$$

$h^h(\theta) \equiv \langle B^2\rangle^{1/2}/B$, and $f_c \equiv 1-f_t$. For the model magnetic field, $\langle B^2\rangle^{1/2} = B_0(1-\epsilon^2)^{-1/4}$ and $h^h = (1-\epsilon)(1-\epsilon^2)^{-1/4}h$.

5. Results

We present the results of the numerical solution using the model magnetic field with circular flux surfaces. First we show the convergence results versus the number of pitch-angle eigenfunctions kept, N, using $\epsilon = 0.3$. For these results, the number of Laguerre polynomials kept is $N+1$, i.e. $L = N$. The results are presented in figure 2. To get within 1% and 0.1% of the $N = 6$ solution (taken to be correct) requires $N = 2$ and $N = 5$ respectively. As required by the variational nature of the problem, the heat flux decreases monotonically as N is increased. The behavior is similar at other ϵ.

We show the heat flux and poloidal flow for several values of ϵ computed with $N = 1$ and $N = 2$ (again $L = N$). In figure 3(*a*) the heat flux is compared with the formulae of Chang–Hinton and Taguchi (we normalize our formulae to use B_0 instead of $B_{\max}$). Those approximate analytical formulae are in good agreement with our exact solution even at finite aspect ratio. In figure 3(*b*) our poloidal flow is compared with the analytic formula derived using Taguchi's method [13]. The analytic formula does reasonably well but can have errors of up to 20% at intermediate aspect ratios. We also observe that our poloidal flow value $\alpha_K^{-1}K$ agrees with figure 8 of [8] when those results at finite aspect ratio are extrapolated to zero collisionality.

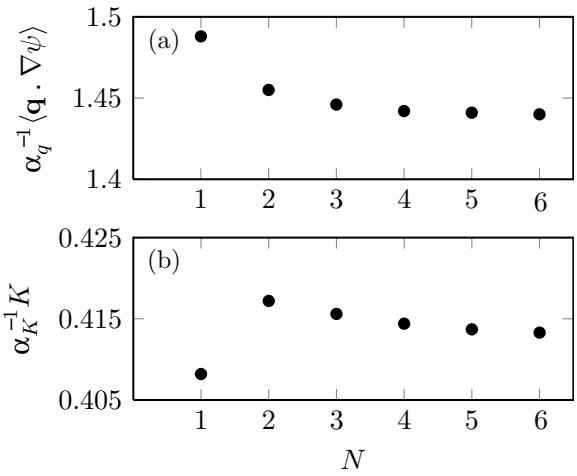

Figure 2. Convergence of the (*a*) heat flux and (*b*) poloidal flow at $\epsilon = 0.3$ as a function of the number of pitch-angle eigenfunctions kept, N. Here we use $L = N$, i.e. one more Laguerre polynomial than pitch-angle eigenfunction.

We have fit our heat flux and poloidal flow curves to polynomials in $\epsilon^{1/2}$ which interpolate over finite aspect ratios. Four terms in each polynomial is adequate:

$$\alpha_q^{-1}\langle \boldsymbol{q}\cdot\nabla\psi\rangle = 1.34\epsilon^{1/2}+2.60\epsilon-2.13\epsilon^{3/2}+3.18\epsilon^2, \tag{65}$$

$$\alpha_K^{-1}K = 1.17-1.22\epsilon^{1/2}-0.68\epsilon+0.72\epsilon^{3/2}. \tag{66}$$

Finally, we show the solution for the distribution function g for several values of ϵ as a function of x at $\lambda = 0.5$ in figure 4(*a*) and as a function of λ at $x = 0.5$ in figure 4(*b*). The full perturbed distribution function is then $f_1 = g + F$, with F given in equation (5). The trend in $g(x,\lambda)$ with ϵ is to decrease in magnitude at small ϵ and increase in magnitude at large ϵ, with the reversal occurring around $\epsilon = 0.5$.

6. Summary

We have developed a method for evaluating neoclassical transport in the core of a tokamak with general magnetic geometry in the low collisionality limit. We have demonstrated that analytic methods which approximate the collision operator are accurate at intermediate aspect ratios for estimating the ion heat flux but can be off by up to 20% at intermediate aspect ratios for estimating the poloidal flow. While we have used circular flux surfaces here, it is straightforward to apply the method to more general geometry. Multiple species could in principle be used as well.

The variational principle we use only applies in the limit of small collisionality and orbit width. When these restrictions are lifted, our technique cannot be used directly in those more general situations where finite collisionality or finite orbit width effects are retained. These important cases must be studied using other means. However, our work efficiently describes the effects of retaining the exact linearized Fokker–Planck collision operator as opposed to common approximations to the collision operator to make the calculations more analytically tractable.

The effectiveness of our calculation is a direct result of using the pitch-angle eigenfunctions associated with

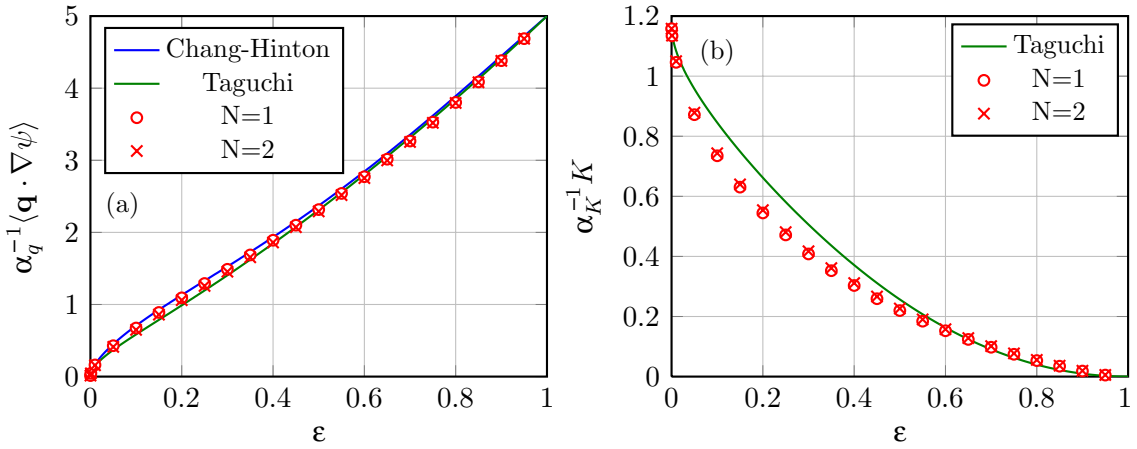

Figure 3. (*a*) Heat flux and (*b*) poloidal flow at several values of ϵ, using $N = 1$ and $N = 2$. Here we use $L = N$, i.e. one more Laguerre polynomial than pitch-angle eigenfunction. The exact numerical solutions are compared with the Chang–Hinton and Taguchi formulae.

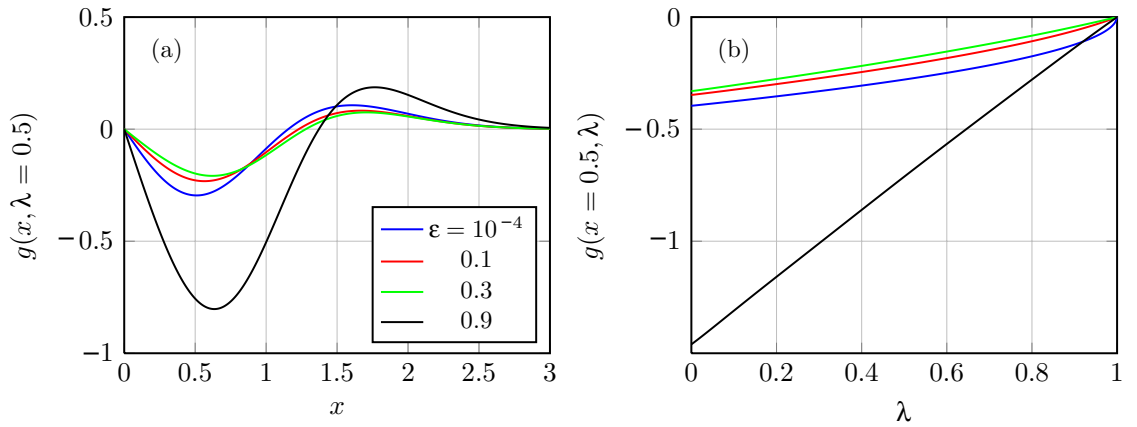

Figure 4. The solution $g(x,\lambda)/(A\kappa)$ is shown for several values of inverse aspect ratio ϵ as (*a*) a function of $x = v/v_T$ at $\lambda = 0.5$ and (*b*) a function of λ at $x = 0.5$. The full perturbed distribution function is $f_1 = g + F$, with F given in equation (5). We show g only for $\sigma = \mathrm{sign}(v_\parallel) = +1$, since g is odd in σ. Here $N = 6$ and $L = N$, i.e. we use one more Laguerre polynomial than pitch-angle eigenfunction. The x dependence is dominated by the first two Laguerre polynomials and the λ dependence is dominated by the first pitch-angle eigenfunction. The trend in $g(x,\lambda)$ with ϵ is to decrease in magnitude at small ϵ and increase in magnitude at large ϵ, with the reversal occurring around $\epsilon = 0.5$.

the transit-averaged test particle collision operator. These eigenfunctions depend on the magnetic geometry, form a complete orthogonal set, and are extremely well suited to this problem, with only one or two basis functions required to obtain an accurate solution.

Acknowledgments

JBP is grateful for the hospitality of the Plasma Science and Fusion Center at MIT, where much of this work was performed. JBP would like to acknowledge support by a US DOE Fusion Energy Sciences Fellowship.

Appendix

A.1. Evaluation of M_{ij}^{Fa}

We simplify equation (53) into a form suitable for numerical integration. The integral is written in coordinates using equation (15). The gyrophase integral over φ_y can be done analytically [16]:

$$I \equiv \int_0^{2\pi} \mathrm{d}\varphi_y\, U(u) = \frac{4(x^2+y^2-2)}{\Lambda}K(\kappa) - 2\Lambda E(\kappa) - \frac{2(x^2-y^2)^2}{\Lambda^3}\frac{E(\kappa)}{1-\kappa^2}, \tag{A1}$$

where here K and E are the complete elliptic integrals of the first and second kind with the modulus as argument, and

$$\Lambda^2 \equiv x^2 + y^2 + 2x_\perp y_\perp - 2x_\parallel y_\parallel, \tag{A2}$$

$$\kappa^2 \equiv \frac{4x_\perp y_\perp}{\Lambda^2}, \tag{A3}$$

$x_\parallel \equiv \sigma_x x\sqrt{1-\lambda_x/h}$, $\sigma_x \equiv \mathrm{sign}(x_\parallel)$, $x_\perp \equiv x\sqrt{\lambda_x/h}$, and similarly for $y_\parallel$ and $y_\perp$. Then let

$$\sum_{\sigma_y} \sigma_y I = \sigma_x I_1(x,\lambda_x,y,\lambda_y,\theta), \tag{A4}$$

where $I_1 \equiv I(\sigma_x = +1, \sigma_y = +1) - I(\sigma_x = +1, \sigma_y = -1)$. We have pulled out a factor of σ_x and evaluated at $\sigma_x = +1$

because the expression is odd in σ_x. Explicitly,

$$I_1 = 4(x^2+y^2-2)\left[\frac{K_+}{\Lambda_+}-\frac{K_-}{\Lambda_-}\right]-2\left[\Lambda_+E_+-\Lambda_-E_-\right] -2(x^2-y^2)^2\left[\frac{E_+}{\Lambda_+^3(1-\kappa_+^2)}-\frac{E_-}{\Lambda_-^3(1-\kappa_-^2)}\right], \tag{A5}$$

where

$$\Lambda_\pm^2 \equiv \Lambda^2(\sigma_x=+1,\sigma_y=\pm1) = x^2+y^2+2xy\left[\sqrt{\frac{\lambda_x\lambda_y}{h^2}}\mp\sqrt{\left(1-\frac{\lambda_x}{h}\right)\left(1-\frac{\lambda_y}{h}\right)}\right], \tag{A6}$$

$$\kappa_\pm^2 \equiv \frac{4xy\sqrt{\lambda_x\lambda_y}}{h\Lambda_\pm^2}, \tag{A7}$$

$$K_\pm \equiv K(\kappa_\pm), \tag{A8}$$

$$E_\pm \equiv E(\kappa_\pm). \tag{A9}$$

The σ_x sum may be performed to gain a factor of 2. Equation (53) becomes

$$M_{ij}^{Fa} = \frac{3}{\sqrt{8}}\left\langle\frac{1}{h^2}\int \mathrm{d}\lambda_x\,\mathrm{d}\lambda_y\,\frac{g_n(\lambda_x)g_{n'}(\lambda_y)}{|\xi_x||\xi_y|}A_{ll'}\right\rangle, \tag{A10}$$

with

$$A_{ll'}(\lambda_x,\lambda_y,\theta) \equiv \int_0^\infty\int_0^\infty \mathrm{d}x\,\mathrm{d}y\,\mathrm{e}^{-(x^2+y^2)} \times x^3y^3L_l^{(3/2)}(x^2)L_{l'}^{(3/2)}(y^2)I_1. \tag{A11}$$

One more integral may be performed analytically by converting to polar coordinates, $x = r\cos\phi$, $y = r\sin\phi$. Then

$$\int_0^\infty \mathrm{d}x\int_0^\infty \mathrm{d}y = \int_0^{\pi/2}\mathrm{d}\phi\int_0^\infty \mathrm{d}r\,r. \tag{A12}$$

Importantly, $\kappa_\pm$ does not depend on r and the r integral is elementary. After some algebra, we have

$$A_{ll'} = \int_0^{\pi/2}\mathrm{d}\phi\,\sin^3 2\phi\,[cC_{ll'}+\mathrm{d}D_{ll'}], \tag{A13}$$

where

$$C_{ll'} \equiv \frac{1}{2^3}\int_0^\infty \mathrm{d}r\,\mathrm{e}^{-r^2}r^6\left[4\left(r^2-2\right)\right]L_l^{(3/2)}\left(r^2\cos^2\phi\right) \times L_{l'}^{(3/2)}\left(r^2\sin^2\phi\right), \tag{A14}$$

$$D_{ll'} \equiv \frac{1}{2^3}\int_0^\infty \mathrm{d}r\,\mathrm{e}^{-r^2}r^6\left(-2r^2\right)L_l^{(3/2)}\left(r^2\cos^2\phi\right) \times L_{l'}^{(3/2)}\left(r^2\sin^2\phi\right), \tag{A15}$$

$$c \equiv \frac{K_+}{L_+}-\frac{K_-}{L_-}, \tag{A16}$$

$$d \equiv (L_+E_+-L_-E_-)+\cos^2 2\phi \times\left[\frac{E_+}{L_+^3(1-\kappa_+^2)}-\frac{E_-}{L_-^3(1-\kappa_-^2)}\right], \tag{A17}$$

$$L_\pm^2 \equiv \Lambda_\pm^2/r^2 = 1+\sin^2 2\phi \times\left[\sqrt{\frac{\lambda_x\lambda_y}{h^2}}\mp\sqrt{\left(1-\frac{\lambda_x}{h}\right)\left(1-\frac{\lambda_y}{h}\right)}\right], \tag{A18}$$

$$\kappa_\pm^2 = \frac{2\sqrt{\lambda_x\lambda_y}\sin 2\phi}{hL_\pm^2}. \tag{A19}$$

After putting the θ integral in explicitly, we finally have

$$M_{ij}^{Fa} = \frac{3}{\sqrt{8}}\int \mathrm{d}\lambda_x\,\mathrm{d}\lambda_y\,g_n(\lambda_x)g_{n'}(\lambda_y)\gamma_{ll'}(\lambda_x,\lambda_y), \tag{A20}$$

where

$$\gamma_{ll'}(\lambda_x,\lambda_y) \equiv \left(\int_0^{2\pi}\frac{\mathrm{d}\theta}{\boldsymbol{B}\cdot\nabla\theta}\right)^{-1} \times\int_0^{2\pi}\mathrm{d}\theta\int_0^{\pi/2}\mathrm{d}\phi\,\frac{\sin^3 2\phi\,[cC_{ll'}+\mathrm{d}D_{ll'}]}{h^2(\boldsymbol{B}\cdot\nabla\theta)|\xi_x||\xi_y|}. \tag{A21}$$

This form is used for numerical integration. The four-dimensional integration is performed using the NAG C Library. The θ and ϕ integrals are computed using two-dimensional adaptive quadrature on a discrete (λ_x,λ_y) grid to give $\gamma_{ll'}$. The eigenfunctions g_n are computed on this grid, and a discrete integration method is used to perform the two λ integrals.

References

[1] Hinton F L and Hazeltine R D 1976 *Rev. Mod. Phys.* **48** 239–308
[2] Hirshman S P and Sigmar D J 1981 *Nucl. Fusion* **21** 1079
[3] Doyle E *et al* 2007 *Nucl. Fusion* **47** S18
[4] Belli E A and Candy J 2008 *Plasma Phys. Control. Fusion* **50** 095010
[5] Belli E A and Candy J 2012 *Plasma Phys. Control. Fusion* **54** 015015
[6] Houlberg W A, Shaing K C, Hirshman S P and Zarnstorff M C 1997 *Phys. Plasmas* **4** 3230–42
[7] Hirshman S P and Sigmar D J 1976 *Phys. Fluids* **19** 1532–40
[8] Wong S K and Chan V S 2011 *Plasma Phys. Control. Fusion* **53** 095005
[9] Rosenbluth M N, Hazeltine R D and Hinton F L 1972 *Phys. Fluids* **15** 116–40
[10] Cordey J 1976 *Nucl. Fusion* **16** 499
[11] Hsu C T, Catto P J and Sigmar D J 1990 *Phys. Fluids* B **2** 280–90
[12] Xiao Y, Catto P J and Molvig K 2007 *Phys. Plasmas* **14** 032302
[13] Helander P and Sigmar D J 2002 *Collisional Transport in Magnetized Plasmas* (Cambridge: Cambridge University Press)
[14] Hinton F L and Rosenbluth M N 1973 *Phys. Fluids* **16** 836–54
[15] 2011 Digital Library of Mathematical Functions. Release date 29 August 2011 National Institute of Standards and Technology from http://dlmf.nist.gov/
[16] Li B and Ernst D R 2011 *Phys. Rev. Lett.* **106** 195002
[17] Chang C S and Hinton F L 1982 *Phys. Fluids* **25** 1493–4
[18] Taguchi M 1988 *Plasma Phys. Control. Fusion* **30** 1897